Molecules **2011**

OPEN ACCESS

molecules

ISSN 1420-3049

www.mdpi.com/journal/molecules

Research

Synthesis, Property Characterization and Photocatalytic Activity of Novel Mulriple Polymer Polyaniline/Bi_2SnTiO_7

Yunjun Yang and Jingfei Luan*

State Key Laboratory of Pollution Control and Resource Reuse, School of the Environment, Nanjing University, Nanjing 210093, China; E-Mail: jfluan@nju.edu.cn

* Author to whom correspondence should be addressed; E-Mail: jfluan@nju.edu.cn; Tel.: +86-135-8520-6718; Fax: +86-25-8370-7304.

Received: / Accepted: / Published:

Abstract: Novel mulriple polymer polyaniline/Bi_2SnTiO_7 was synthesized by chemical oxidation in-situ polymerization method and sol-gel method for the first time. The structural and photocatalytic properties of novel polyaniline/Bi_2SnTiO_7 have been characterized by

X-ray diffraction, scanning electron microscopy, X-ray photoelectron spectroscopy and X-ray spectrometry. The lattice parameter of Bi_2SnTiO_7 was found to be a = 10.52582(8) Å. The photocatalytic degradation of methylene blue was realized under visible light irradiation with novel polyaniline/Bi_2SnTiO_7 as catalyst. The results showed that novel polyaniline/Bi_2SnTiO_7 owned higher catalytic activity compared with Bi_2InTaO_7 or pure TiO_2 or N-doped TiO_2 for photocatalytic degradation of methylene blue under visible light irradiation. The photocatalytic degradation of methylene blue with novel polyaniline/Bi_2SnTiO_7 or N-doped TiO_2 as catalyst followed the first-order reaction kinetics, and the first-order rate constant was 0.01504 min^{-1} or 0.00333 min^{-1}. After visible light irradiation for 220 min with novel polyaniline/Bi_2SnTiO_7 as catalyst, complete removal and mineralization of methylene blue was observed. The reduction of the total organic carbon, the formation of inorganic products, SO_4^{2-} and NO_3^-, and the evolution of CO_2 revealed the continuous mineralization of methylene blue during the photocatalytic process. The possible photocatalytic degradation pathway of methylene blue was obtained under visible light irradiation. Novel mulriple polymer polyaniline/Bi_2SnTiO_7/(visible light) photocatalysis system was found to be suitable for textile industry wastewater treatment and could be used to solve other environmental chemical pollution problems.

Keywords: Polyaniline/Bi_2SnTiO_7; synthesis; property; photocatalytic activity; methylene blue; visible light irradiation; photodegradation pathway

1. Introduction

Dye effluents which came from textile industries were becoming a serious environmental problem because of their toxicity, high chemical oxygen demand content, and biological degradation [1]. A lot of conventional methods had been proposed to treat industrial effluents, but each method had its shortcomings [1-7]. In the last decade, photocatalytic degradation processes had been widely applied as techniques of destruction of organic pollutants in wastewater and effluents, especially degradation of dyes [1, 7-21]. Among various dyes, methylene blue (MB) dye was difficult to be degraded and was often used as a model dye contaminant to evaluate the activity of a photocatalyst both under ultraviolet light irradiation [18, 19, 22] and under visible light irradiation [20, 21, 23, 24]. There were a lot of reports on the photodegradation of MB. Unfortunately, most of these reports were carried out under UV light irradiation. Up to now, there were only few reports of MB dye degradation under visible light irradiation such as the research from Asahi et al. with a reduced TiO_x ($TiO_{2-x}N_x$) as catalyst and the research from Li et al. with Pt–TiO_2 as photocatalyst [21,24]. Zhang [25] utilized N-doped TiO_2 as catalyst to degrade MB under visible light irradiation and found that the removal ratio of MB was only 35% after visible light irradiation for 180 min. It was known that ultraviolet light only occupied 4% of the solar energy. For this reason, large numbers of endeavors should be taken up with developing new visible light-responsive photocatalysts which were capable of utilizing more ample visible light, which occupied about 43% of the solar energy. Therefore, it was urgent to develop novel visible light-responsive photocatalysts.

With the development of investigation of photocatalysis process, investigators also paid much attention to researching and developing novel photocatalysts [26-29]. Recently, TiO_2 was the most common photocatalyst. However, TiO_2 could not be utilized in the visible light region and could only degrade MB under ultraviolet light irradiation. Therefore, some efficient catalysts which could generate electron-hole pairs under visible light irradiation should be developed. Fortunately, $A_2B_2O_7$ compounds were often considered to have photocatalytic properties under visible light irradiation. In our previous work [30], we had found that Bi_2InTaO_7 crystallized with the pyrochlore-type structure and acted as a photocatalyst under visible light irradiation and seemed to have potential for improvement of photocatalytic activity by modification of its structure. According to above analysis, we could assume that substitution of Ta^{5+} and In^{3+} by Sn^{4+} and Ti^{4+} in Bi_2InTaO_7 might increase carriers concentration. As a result, a change and improvement of the electrical transportation and photophysical properties could be found in the novel Bi_2SnTiO_7 compound which might own advanced photocatalytic properties. Moreover, due to the excellent environmental stability of polyaniline, the polyaniline-hybridized Bi_2SnTiO_7 sample should own more advanced photocatalytic properties.

Bi_2SnTiO_7 had never been produced and the data about its structural and photophysical properties such as space group and lattice constants had not been found previously. In addition, the photocatalytic properties of Bi_2SnTiO_7 had not been studied by other investigators. The molecular composition of Bi_2SnTiO_7 was very similar with other $A_2B_2O_7$ compounds. Thus the resemblance suggested that Bi_2SnTiO_7 and the polyaniline-hybridized

Bi_2SnTiO_7 might possess photocatalytic properties under visible light irradiation, which was similar with other members in $A_2B_2O_7$ family. Bi_2SnTiO_7 also seemed to have potential for improvement of photocatalytic activity by modification of its structure because it had been proved that a slight modification of a semiconductor structure would result in a remarkable change in photocatalytic properties [21]. In this paper, Bi_2SnTiO_7 was prepared for the first time by the solid-state reaction method and the novel mulriple polymer polyaniline/Bi_2SnTiO_7 was synthesized by chemical oxidation in-situ polymerization method and sol-gel method for the first time. The structure and photocatalytic properties of the polyaniline-hybridized Bi_2SnTiO_7 were investigated in detail. The photocatalytic degradation of MB under visible light irradiation was also performed to evaluate the photocatalytic activity of the polyaniline-hybridized Bi_2SnTiO_7. A comparison between the photocatalytic properties of the polyaniline-hybridized Bi_2SnTiO_7, Bi_2InTaO_7 and N-doped TiO_2 was achieved in order to elucidate the structure-photocatalytic activity relationship in the polyaniline-hybridized Bi_2SnTiO_7.

2. Experimental

2.1. Synthesis of the Polyaniline-hybridized Bi_2SnTiO_7 and N-doped TiO_2

Bi_2SnTiO_7 powder was first synthesized by the solid-state reaction method. TiO_2, SnO_2, Bi_2O_3, In_2O_3 and Ta_2O_5 with the purity of 99.99% were utilized as raw materials which were purchased from Sinopharm Group Chemical Reagent Co. (Shanghai, China) and used without further purification. All powders were dried at 200 ℃ for 4 h before synthesis. In order to synthesize Bi_2SnTiO_7, the precursors were stoichiometrically mixed in a quartz mortar,

subsequently pressed into small columns and put into an alumina crucible (Shenyang Crucible Co., LTD, China). Finally, calcination was carried out at 1100 ^{o}C for 30 h in an electric furnace (KSL 1700X, Hefei Kejing Materials Technology CO., LTD, China). Similarly, Bi_2InTaO_7 was synthesized by calcination at 1050 ^{o}C for 46 h. After sintering and grounding within a quartz mortar, ultrafine Bi_2SnTiO_7 powder was fabricated.

A polyaniline-hybridized Bi_2SnTiO_7 sample was prepared as follows: an amount of distilled aniline was added to 150 mL of 1M HCl, and subsequently stirred for 30 min to ensure that the aniline was totally dissolved. Subsequently, certain percentage of Bi_2SnTiO_7 was added into above solution, sonicated for 30 min to obtain dispersed solution, and then stirred for 1 h. Thirdly, 0.5 g mL^{-1} ammonium thiosulphate (HCl) was added into the solution slowly, then the mixture was stirred for 24 h. Finally, the suspension was filtered, and the precipitate was washed with alcohol and water for many times and dried at 60 °C to obtain polyaniline-hybridized-Bi_2SnTiO_7 .

Nitrogen-doped titania (N-doped TiO_2) catalyst with tetrabutyl titanate as a titanium precursor was prepared by using the sol–gel method at room temperature. The following procedure was that 17 mL tetrabutyl titanate and 40mL absolute ethyl alcohol were mixed as solution a, subsequently solution a was added dropwise under vigorous stirring into the solution b that contained 40 mL absolute ethyl alcohol, 10 mL glacial acetic acid and 5 mL double distilled water to form transparent colloidal suspension c. Subsequently aqua ammonia with N/Ti proportion of 8 mol% was added into the resulting transparent colloidal suspension under

vigorous stirring and stirred for 1 h. Finally, the xerogel was formed after being aged for 2 days. The xerogel was ground into powder which was calcined at 500 ˚C for 2 h, subsequently above powder was ground in agate mortar and screened by shaker to obtain N-doped TiO_2 powders.

2.2. Characterization of the Polyaniline-hybridized Bi_2SnTiO_7

The crystalline phase of Bi_2SnTiO_7 was analyzed by X-ray diffractometer (D/MAX-RB, Rigaku Corporation, Japan) with Cu$K\alpha$ radiation (λ = 1.54056). The patterns were collected at 295 K with a step-scan procedure in the range of 2θ = 10-100°. The step interval was 0.02° and the time per step was 1.2 s. The accelerating voltage and applied current were 40 kV and 40 mA, respectively. The chemical composition of the compound was determined by scanning electron microscope-X-ray energy dispersion spectrum (SEM-EDS, LEO 1530VP, LEO Corporation, Germany), X-ray fluorescence spectrometer (XFS, ARL-9800, ARL Corporation, Switzerland) and X-ray photoelectron spectroscopy (XPS, ESCALABMK-2, VG Scientific Ltd., U.K.). The particle morphology of Bi_2SnTiO_7 was measured by transmission electron microscope (Tecnal F20 S-Twin, FEI Corporation, USA). The Bi^{3+} content, Sn^{4+} content, Ti^{4+} content and O^{2-} content of Bi_2SnTiO_7 and the valence state of elements were also analyzed by X-ray photoelectron spectroscopy (XPS). The chemical composition within the depth profile of Bi_2SnTiO_7 was examined by the argon ion denudation method when X-ray photoelectron spectroscopy was utilized. The surface areas of Bi_2SnTiO_7 and N-doped TiO_2 were measured by the Brunauer-Emmett-Teller (BET) method (MS-21, Quantachrome Instruments Corporation, USA) with N_2 adsorption at liquid nitrogen temperature. The particle sizes of the

photocatalysts were measured by Malvern's mastersize-2000 particle size analyzer (Malvern Instruments Ltd, United Kingdom).

2.3. Photocatalytic Activity Tests

The photocatalytic activity of the polyaniline-hybridized Bi_2SnTiO_7 was evaluated with methylene blue ($C_{16}H_{18}ClN_3S$) (Tianjin Bodi Chemical Co., Ltd., China) as a model material. The photoreaction was carried out in a photochemical reaction apparatus (Nanjing Xujiang Machine Plant, China). The internal structure of the reaction apparatus is as following: the lamp is put into a quartz hydrazine which is a hollow structure and located in the middle of the reactor. The recycling water through the reactor maintains a near constant reaction temperature (20 ℃) and the solution was continuously stirred and aerated. Twelve holes which were utilized to put quartz tubes evenly distribute around the lamp and the distance between the lamp and each hole was equal. Under the condition of magnetic stirring, the photocatalyst within the MB solution was in the state of suspension. In this paper, the photocatalytic degradation of the MB solution was performed with 0.3 g polyaniline-hybridized Bi_2SnTiO_7 in 300 mL 0.025 mM MB aqueous solution in quartz tubes with 500 W Xenon lamp (400 nm $<\lambda <$ 800 nm) as visible-light source. Prior to visible light irradiation, the suspensions which contained the catalyst and MB dye were magnetically stirred in the dark for 45 min to ensure establishment of an adsorption/desorption equilibrium among the polyaniline-hybridized Bi_2SnTiO_7, the MB dye and atmospheric oxygen. During visible light illumination, the suspension was stirred at 500 rpm and the initial pH value of the MB solution was 7.0 without pH adjustment in the reaction process. Above experiments were performed under

oxygen-saturation conditions ($[O_2]_{sat} = 1.02 \times 10^{-3}$ M). One of the quartz tubes was taken out from the photochemical reaction apparatus at various time intervals. The suspension was filtered through 0.22 μm membrane filters. The filtrate was subsequently analyzed by a Shimadzu UV-2450 UV-Visible spectrometer with the detecting wavelength at 665 nm. The experimental error was found to be within ±2.2%.

The incident photon flux I_o measured by a radiometer (Model FZ-A, Photoelectric Instrument Factory Beijing Normal University, China) was determined to be 4.76×10^{-6} Einstein L^{-1} s^{-1} under visible light irradiation (wavelength range of 400-700 nm). The incident photon flux on the photoreactor was varied by adjusting the distance between the photoreactor and the Xe arc lamp. pH adjustment was not carried out and the initial pH value was 7.0. The inorganic products which were obtained from MB degradation were analyzed by ion chromatograph (DX-300, Dionex Corporation, USA). The identification of MB and the degradation intermediate products of MB were performed by liquid chromatograph—mass spectrometer (LC-MS, Thermo Quest LCQ Duo, USA, Beta Basic-C_{18} HPLC column: 150 × 2.1 mm, ID of 5 μm, Finnigan, Thermo, USA). Here, 20 μL of post-photocatalysis solution was injected automatically into the LC-MS system. The fluent contained 60% methanol and 40% water, and the flow rate was 0.2 mL min^{-1}. MS conditions included an electrospray ionization interface, a capillary temperature of 27 ℃ with a voltage of 19.00 V, a spray voltage of 5000 V and a constant sheath gas flow rate. The spectrum was acquired in the negative ion scan mode and the $m\ z^{-1}$ range swept from 50 to 600. Evolution of CO_2 was analyzed with an intersmat™ IGC120-MB gas chromatograph equipped with a porapack Q column (3 m in length and an

inner diameter of 0.25 in.), which was connected to a catharometer detector. The total organic carbon (TOC) concentration was determined with a TOC analyzer (TOC-5000, Shimadzu Corporation, Japan). The photonic efficiency was calculated according to the following equation: [31, 32]

$$\varphi = R/I_o \quad (1)$$

where φ was the photonic efficiency (%), R was the rate of MB degradation (Mol L^{-1} s^{-1}), and I_o was the incident photon flux (Einstein L^{-1} s^{-1}).

3. Results and Discussion

3.1. Crystal Structure of Bi_2SnTiO_7

Figure 1 presents TEM image and the selected area electron diffraction pattern of Bi_2SnTiO_7. The TEM image of Bi_2SnTiO_7 showed that the morphology of the Bi_2SnTiO_7 particle was very similar and regular. It could be seen that the Bi_2SnTiO_7 particles crystallited well and the average particle size of Bi_2SnTiO_7 was about 180 nm. SEM-EDS spectrum of Bi_2SnTiO_7 revealed that Bi_2SnTiO_7 was pure phase without any other impure elements and Bi_2SnTiO_7 displayed the presence of bismuth, tin, titanium and oxygen. It could be seen from Figure 1 that Bi_2SnTiO_7 crystallized with the pyrochlore-type structure, cubic crystal system and space group *Fd3m*. The lattice parameter for Bi_2SnTiO_7 was proved to be a = 10.52582(8) Å. According to the calculation results from Figure 1, the (h k l) value for the main peaks of Bi_2SnTiO_7 could be found and indexed.

Full-profile structure refinements of the collected X-ray diffraction data of Bi_2SnTiO_7 were obtained by the RIETAN^{TM} [33] program, which was based on Pawley analysis. The refinement results of Bi_2SnTiO_7 are shown in Figure 2. The atomic coordinates and structural parameters of Bi_2SnTiO_7 are listed in Table 1. The results of the final refinement for Bi_2SnTiO_7 indicated a good agreement between the observed and calculated intensities in a pyrochlore-type structure and cubic crystal system with space group *Fd3m*. Our XRD results also showed that Bi_2SnTiO_7 and Bi_2InTaO_7 crystallized in the same structure, and 2 theta angles of each reflection of Bi_2SnTiO_7 changed with Sn^{4+} and Ti^{4+} being replaced by In^{3+} and Ta^{5+}. Bi_2InTaO_7 also crystallized with a cubic structure by space group Fd3m and the lattice parameter of Bi_2InTaO_7 was a = 10.74641(0) Å. The lattice parameter of Bi_2SnTiO_7 was a = 10.52582(8) Å, which indicated that the lattice parameter of Bi_2SnTiO_7 decreased compared with the lattice parameter of Bi_2InTaO_7 because the In^{3+} ionic radii (0.92 Å) was larger than the Sn^{4+} ionic radii (0.71Å) and the Ta^{5+} ionic radii (0.68 Å) was equal to the Ti^{4+} ionic radii (0.68Å). The outcome of refinement for Bi_2SnTiO_7 generated the unweighted *R* factor, R_P = 10.72% with space group *Fd3m*. Zou *et al.* [34] refined the crystal structure of Bi_2InNbO_7 and obtained a large *R* factor for Bi_2InNbO_7, which was ascribed to a slightly modified structure model for Bi_2InNbO_7. According to the high purity of the precursors which were utilized in this study and the EDS results that did not trace any other elements, it was unlikely that the observed space groups originated from the presence of impurities. Therefore, it was suggested that the slightly high *R* factor for Bi_2SnTiO_7 was owing to a slightly modified structure model for Bi_2SnTiO_7. It should be emphasized that the defects or the disorder/order of a fraction of

the atoms could cause the change of structures, including different bond-distance distributions, thermal displacement parameters and/or occupation factors for some of the atoms.

In order to reveal the surface chemical compositions and the valence states of various elements of Bi_2SnTiO_7, the X-ray photoelectron spectrum of Bi_2SnTiO_7 for detecting Bi, Sn, Ti and O was performed. The full XPS spectrum confirmed that the prepared Bi_2SnTiO_7 contained elements of Bi, Sn, Ti and O, which was consistent with the results of SEM-EDS. The different elemental peaks for Bi_2SnTiO_7 which are corresponding to definite bind energies are given in Table 2. The results illustrated that the oxidation states of Bi, Sn, Ti and O ions from Bi_2SnTiO_7 were +3, +4, +4 and -2, respectively. Moreover, the average atomic ratio of Bi: Sn: Ti: O for Bi_2SnTiO_7 was 2.00: 0.98: 1.02: 6.97 accoring to our XPS, SEM-EDS and XFS results. Accordingly, it could be deduced that the resulting material was highly pure under our preparation conditions. It was remarkable that there were not any shoulders and widening in the XPS peaks of Bi_2SnTiO_7, which suggested the absence of any other phases.

3.2. Photocatalytic Properties

Generally, the direct absorption of band-gap photons would result in the generation of electron–hole pairs within the polyaniline-hybridized Bi_2SnTiO_7, subsequently, the charge carriers began to diffuse to the surface of the polyaniline-hybridized Bi_2SnTiO_7. As a result, the photocatalytic activity for decomposing organic compounds with the polyaniline-hybridized Bi_2SnTiO_7 might be enhanced. Changes in the UV-Vis spectrum of MB upon exposure to visible light (λ > 400 nm) irradiation with the presence of the

polyaniline-hybridized Bi_2SnTiO_7, Bi_2InTaO_7 or N-doped TiO_2 indicated that the polyaniline-hybridized Bi_2SnTiO_7, Bi_2InTaO_7 or N-doped TiO_2 could photodegrade MB effectively under visible light irradiation. Figure 3 shows the photocatalytic degradation of methylene blue under visible light irradiation in the presence of the polyaniline-hybridized Bi_2SnTiO_7, Bi_2InTaO_7, pure TiO_2, N-doped TiO_2 as well as in the absence of a photocatalyst. The results showed that a reduction in typical MB peaks at 665 nm and 614 nm was clearly noticed and the photodegradation rate of MB was about 2.046×10^{-9} mol L^{-1} s^{-1} and the photonic efficiency was estimated to be 0.0430% (λ = 420 nm) with the polyaniline-hybridized Bi_2SnTiO_7 as catalyst. Similarly, the photodegradation rate of MB was about 1.001×10^{-9} mol L^{-1} s^{-1} and the photonic efficiency was estimated to be 0.0210% (λ = 420 nm) with N-doped TiO_2 as catalyst. Furthermore, the photodegradation rate of MB was about 0.891×10^{-9} mol L^{-1} s^{-1} and the photonic efficiency was estimated to be 0.0187% (λ = 420 nm) with Bi_2InTaO_7 as catalyst. As a contradistinction, the photodegradation rate of MB within 200 minutes of visible light irradiation was only 0.8338×10^{-9} mol L^{-1} s^{-1} and the photonic efficiency was estimated to be 0.0175% (λ = 420 nm) with pure TiO_2 as catalyst. The photodegradation rate of MB was about 0.6830×10^{-9} mol L^{-1} s^{-1} and the photonic efficiency was estimated to be 0.0143% (λ = 420 nm) in the absence of a photocatalyst. The results showed that the photodegradation rate of MB and the photonic efficiency with the polyaniline-hybridized Bi_2SnTiO_7 as catalyst were both higher than those with N-doped TiO_2 or Bi_2InTaO_7 or pure TiO_2 as catalyst. The photodegradation rate of MB and the photonic efficiency with N-doped TiO_2 as catalyst were both higher than those with Bi_2InTaO_7 or pure TiO_2 as catalyst. The photodegradation rate of MB and the photonic efficiency with Bi_2InTaO_7 as catalyst were both

higher than those with pure TiO_2 or the absence of a photocatalyst. The photodegradation rate of MB and the photonic efficiency with pure TiO_2 as catalyst were both higher than those with the absence of a photocatalyst. When the polyaniline-hybridized Bi_2SnTiO_7, N-doped TiO_2, Bi_2InTaO_7 or pure TiO_2 was utilized as photocatalyst, the photodegradation conversion rate of MB was 98.20%, 48.05%, 42.76% and 40.02% after visible light irradiation for 200 minutes, respectively. Furthermore, the photodegradation conversion rate of MB was 32.78% after visible light irradiation for 200 minutes with the absence of a photocatalyst because of the MB dye photo-sensitization effect [35]. After visible light irradiation for 220 minutes with the polyaniline-hybridized Bi_2SnTiO_7 as catalyst, complete removal of MB was observed and the complete disappearance of the absorption peaks which presented the absolute color change from deep blue into colorless solution occurred. According to above results, the photocatalytic degradation activity of the polyaniline-hybridized Bi_2SnTiO_7 was much higher than that of N-doped TiO_2, Bi_2InTaO_7 or pure TiO_2. Meanwhile, N-doped TiO_2 showed higher photocatalytic degradation activity for MB photodegradation compared with Bi_2InTaO_7 or pure TiO_2. Bi_2InTaO_7 showed higher photocatalytic degradation activity for MB photodegradation compared with pure TiO_2. Pure TiO_2 was more suitable for MB photodegradation than the absence of a photocatalyst. The photocatalytic property of novel polyaniline-hybridized Bi_2SnTiO_7 under visible light irradiation was amazing compared with that of N-doped TiO_2 or pure TiO_2, and the main reason was that the specific surface area of the polyaniline-hybridized Bi_2SnTiO_7 was much smaller than that of N-doped TiO_2 or pure TiO_2. BET isotherm measurements of the polyaniline-hybridized Bi_2SnTiO_7, N-doped TiO_2 and pure TiO_2 provided a specific surface area of 4.29 $m^2 g^{-1}$, 45.53 $m^2 g^{-1}$ and 46.24 $m^2 g^{-1}$

respectively, which indicated that the photocatalytic degradation activity of the polyaniline-hybridized Bi_2SnTiO_7 could be improved consumedly by enhancing the specific surface area of the polyaniline-hybridized Bi_2SnTiO_7.

Figure 4 shows the change of TOC during photocatalytic degradation of MB with the polyaniline-hybridized Bi_2SnTiO_7, Bi_2InTaO_7 or N-doped TiO_2 as catalyst under visible light irradiation. The TOC measurements revealed the disappearance of organic carbon when the MB solution which contained the polyaniline-hybridized Bi_2SnTiO_7, Bi_2InTaO_7 or N-doped TiO_2 was exposed under visible light irradiation. The results showed that 96.77% or 46.77% or 41.71% of TOC decrease was obtained after visible light irradiation for 200 min when the polyaniline-hybridized Bi_2SnTiO_7 or N-doped TiO_2 or Bi_2InTaO_7 was utilized as photocatalyst. Consequently, after visible light irradiation for 220 min with the polyaniline-hybridized Bi_2SnTiO_7 as catalyst, the entire mineralization of MB was observed because of 100% TOC removal. The turnover number which represented the ratio between the total amount of evolved gas and dissipative catalyst was calculated to be more than 0.258 for the polyaniline-hybridized Bi_2SnTiO_7 after 200 minutes of reaction time under visible light irradiation and this turnover number was evident to prove that this reaction occurred catalytically. Similarly, when the light was turned off in this experiment, the stop of this reaction showed the obvious light response.

Figure 5 shows the amount of CO_2 which was yielded during the photodegradation of MB with the polyaniline-hybridized Bi_2SnTiO_7, Bi_2InTaO_7 or N-doped TiO_2 as catalyst under visible light irradiation. The amount of CO_2 increased gradually with increasing reaction time

when MB was photodegraded by the polyaniline-hybridized Bi_2SnTiO_7, Bi_2InTaO_7 or N-doped TiO_2. At the same time, after visible light irradiation of 200 minutes, the CO_2 production of 0.11129 mmol with the polyaniline-hybridized Bi_2SnTiO_7 as catalyst was higher than the CO_2 production of 0.05600 mmol with N-doped TiO_2 as catalyst. Meanwhile after visible light irradiation of 200 minutes, the CO_2 production of 0.05600 mmol with N-doped TiO_2 as catalyst was higher than the CO_2 production of 0.04934 mmol with Bi_2InTaO_7 as catalyst.

The first-order nature of the photocatalytic degradation kinetics with the polyaniline-hybridized Bi_2SnTiO_7 or Bi_2InTaO_7 or N-doped TiO_2 as catalyst is clearly demonstrated in Figure 6. The results showed a linear correlation between ln (C/C_o) (or ln (TOC/TOC_o)) and the irradiation time for the photocatalytic degradation of MB under visible light irradiation with the presence of the polyaniline-hybridized Bi_2SnTiO_7 or Bi_2InTaO_7 or N-doped TiO_2. Here, C represented the MB concentration at time t, and C_o represented the initial MB concentration, and TOC represented the total organic carbon concentration at time t, and TOC_o represented the initial total organic carbon concentration. According to Figure 6, the first-order rate constant k_C of MB concentration was estimated to be 0.01504 min^{-1} with the polyaniline-hybridized Bi_2SnTiO_7 as catalyst, 0.00275 min^{-1} with Bi_2InTaO_7 as catalyst and 0.00333 min^{-1} with N-doped TiO_2 as catalyst. The different value of k_C indicated that the polyaniline-hybridized Bi_2SnTiO_7 was more suitable for the photocatalytic degradation of MB under visible light irradiation than N-doped TiO_2 or Bi_2InTaO_7. Meanwhile N-doped TiO_2 was more suitable for the photocatalytic degradation of MB under visible light irradiation than

Bi_2InTaO_7. Figure 6 also showed that the first-order rate constant K_{TOC} of TOC was estimated to be 0.01290 min^{-1} with the polyaniline-hybridized Bi_2SnTiO_7 as catalyst, 0.00275 min^{-1} with N-doped TiO_2 as catalyst and 0.00259 min^{-1} with Bi_2InTaO_7 as catalyst, which indicated that the photodegradation intermediate products of MB probably appeared during the photocatalytic degradation of MB under visible light irradiation because of the different value between k_C and K_{TOC}. It could also be seen from Figure 6 that the polyaniline-hybridized Bi_2SnTiO_7 showed higher mineralization efficiency for MB degradation compared with N-doped TiO_2 or Bi_2InTaO_7. At the same time, N-doped TiO_2 showed higher mineralization efficiency for MB degradation compared with Bi_2InTaO_7.

Some inorganic ions such as NH_4^+, NO_3^- and SO_4^{2-} were formed in parallel as the end products of nitrogen and sulfur atoms which existed in MB. Figure 7 and Figure 8 shows the concentration variation of SO_4^{2-} and NO_3^- during photocatalytic degradation of MB with the polyaniline-hybridized Bi_2SnTiO_7 or Bi_2InTaO_7 or N-doped TiO_2 as catalyst under visible light irradiation. The results showed that the concentration of NO_3^- or SO_4^{2-} increased gradually with increasing reaction time when MB was photodegraded by the polyaniline-hybridized Bi_2SnTiO_7 or Bi_2InTaO_7 or N-doped TiO_2. Monitoring the presence of ions in the solution revealed that the SO_4^{2-} ion concentration was 0.01714 mM or 0.00924 mM or 0.00757 mM with the polyaniline-hybridized Bi_2SnTiO_7 or N-doped TiO_2 or Bi_2InTaO_7 as catalyst after visible light irradiation for 200 minutes, indicating that 68.56% or 36.94% or 30.28% of sulfur from MB was converted into sulfate ions with the polyaniline-hybridized Bi_2SnTiO_7 or N-doped TiO_2 or Bi_2InTaO_7 as catalyst after visible light irradiation for 200 minutes. It could

be seen from Figure 8 that the NO_3^- ion concentration was 0.07165 mM or 0.0351 mM or 0.02232 mM with the polyaniline-hybridized Bi_2SnTiO_7 or N-doped TiO_2 or Bi_2InTaO_7 as catalyst after visible light irradiation for 200 minutes, indicating that 95.53% or 46.80% or 29.76% of nitrogen from MB was converted into nitrate ions with the polyaniline-hybridized Bi_2SnTiO_7 or N-doped TiO_2 or Bi_2InTaO_7 as catalyst after visible light irradiation for 200 minutes. The sulfur was first hydrolytically removed, and subsequently was oxidized and transformed into SO_4^{2-}. At the same time, nitrogen atoms in the −3 oxidation state prduced NH_4^+ cations that subsequently were oxidized into NO_3^- ions. As expected, the formation kinetics with the polyaniline-hybridized Bi_2SnTiO_7 was significantly faster than that of N-doped TiO_2 or Bi_2InTaO_7 by using the same amount of photocatalyst. Moreover, the formation kinetics with N-doped TiO_2 was faster than that of Bi_2InTaO_7 by using the same amount of photocatalyst. It was noteworthy that the amount of SO_4^{2-} ions which was released into the solution was lower than the amount of SO_4^{2-} which should come from stoichiometry. One possible reason could be a loss of sulfur-containing volatile compounds such as SO_2. The second possible reason was a partially irreversible adsorption of some SO_4^{2-} ions on the surface of the photocatalyst which had been observed by Lachheb et al. by titanium dioxide [36]. Regardless whether the sulfate ions were adsorbed irreversibly on the surface or not, it was important to stress that the evidence for restrained photocatalytic activity was not noticed.

The photodegradation intermediate products of MB in our experiment were identified as azure B, azure C, thionine, phenothiazine, leucomethylene blue,

N,*N*-dimethyl*p*-phenylenediamine, phenol and aniline. According to the intermediate products which were found in this work and the observed appearance time of other intermediate products, a possible photocatalytic degradation pathway for MB was proposed. Figure 9 shows the suggested photocatalytic degradation pathway scheme for methylene blue under visible light irradiation in the presence of the polyaniline-hybridized Bi_2SnTiO_7. The molecule of MB was converted to small organic species, which were subsequently mineralized into inorganic products such as SO_4^{2-} ions, NO_3^- ions, CO_2 and water ultimately.

3.3. Photocatalytic Degradation Mechanism

The action spectra of MB degradation with the polyaniline-hybridized Bi_2SnTiO_7 as catalyst was observed under visible light irradiation. A clear photonic efficiency (0.0112% at its maximal point) at wavelengths which corresponded to sub-Eg energies of the photocatalysts (λ from 490 nm to 800 nm) was observed for the polyaniline-hybridized Bi_2SnTiO_7. The existence of photonic efficiency at this region revealed that photons were not absorbed by the photocatalysts. In particular, the correlation between the low-energy action spectrum and the absorption spectrum of MB clearly demonstrated that any photodegradation results at wavelengths above 490 nm should be attributed to photosensitization effect by the dye MB itself (Scheme I).

Scheme I:

$$MB_{(ads)} \xrightarrow{\text{Visible light}} MB^*_{(ads)} \quad (2)$$

$$MB^*_{(ads)} + \text{Polyaniline-hybridized } Bi_2SnTiO_7 \rightarrow Fe_2BiSbO_7\ (e) + MB^+_{(ads)} \quad (3)$$

$$\text{Polyaniline-hybridized } Bi_2SnTiO_7\ (e) + O_2 \rightarrow \text{Polyaniline-hybridized } Bi_2SnTiO_7 + \cdot O_2^- \quad (4)$$

According to the mechanism which was shown in Scheme I, MB which was adsorbed on the polyaniline-hybridized Bi_2SnTiO_7 was excited by visible light irradiation. Subsequently, an electron was injected from the excited MB to the conduction band of the polyaniline-hybridized Bi_2SnTiO_7 where the electron was scavenged by molecular oxygen. Scheme I explained the results which were obtained with the polyaniline-hybridized Bi_2SnTiO_7 as catalyst under visible light irradiation, where the polyaniline-hybridized Bi_2SnTiO_7 could serve to reduce recombination of photogenerated electrons and holes by scavenging of electrons [37].

Below 490 nm, the situation was different. The results of photonic efficiency correlated well with the absorption spectra of the polyaniline-hybridized Bi_2SnTiO_7. These results evidently showed that the mechanism which was responsible for the photodegradation of MB went through band gap excitation of the polyaniline-hybridized Bi_2SnTiO_7. Despite the detailed experiments about the effect of oxygen and water were not performed, it was logical to presume that the mechanism in the first step was similar to the observed mechanism for the polyaniline-hybridized Bi_2SnTiO_7 under supra-bandgap irradiation, namely Scheme II:

Scheme II:

$$\text{Polyaniline-hybridized } Bi_2SnTiO_7 \xrightarrow{\text{Visible light}} h^+ + e^- \quad (5)$$

$$e^- + O_2 \rightarrow \cdot O_2^- \quad (6)$$

$$h^+ + OH^- \rightarrow \cdot OH \quad (7)$$

According to first principles calculations, we deduced that the conduction band of the polyaniline-hybridized Bi_2SnTiO_7 was composed of Ti 3*d* and Sn 5*p* orbital component, and the valence band of the polyaniline-hybridized Bi_2SnTiO_7 was composed of O 2*p* and Bi 6*s* orbital component. The polyaniline-hybridized Bi_2SnTiO_7 could produce electron–hole pairs by absorption of photons directly, and it indicated that enough energy which was larger than the band gap energy of the polyaniline-hybridized Bi_2SnTiO_7 was necessary for the photocatalytic degradation process of MB.

Former luminescent studies had shown that the closer the M–O–M bond angle was to 180°, the more delocalized was the excited state [38]. As a result, the charge carriers could move more easily in the matrix. The mobility of the photoinduced electrons and holes influenced the photocatalytic activity because high diffusivity indicated the enhancement of probability that the photogenerated electrons and holes would reach the reactive sites of the catalyst surface. According to above results, the lattice parameter a =10.52582(8) Å for Bi_2SnTiO_7 was smaller than the lattice parameter α = 10.70352(7) Å for Bi_2InTaO_7, thus the photoinduced electrons and holes inside Bi_2SnTiO_7 was easier and faster to reach the reactive sites on the catalyst surface compared with those of Bi_2InTaO_7, which showed the photocatalytic degradation activity of Bi_2SnTiO_7 was higher than that of Bi_2InTaO_7. For the polyaniline-hybridized Bi_2SnTiO_7 in this experiment, the Sn–O–Ti bond angle was 140.196^o and the In–O–Ta bond angle was 118.764^o, indicating that the Sn–O–Ti or In–O–Ta bond angle was close to 180^0. Thus the photocatalytic activity of the polyaniline-hybridized Bi_2SnTiO_7 was correspondingly higher. The crystal structures of Bi_2SnTiO_7 and Bi_2InTaO_7 were the same, but their electronic

structures were considered to be somewhat different. For Bi_2SnTiO_7, Ti was 3*d*-block metal element, and Bi was 6*p*-block rare earth metal element, and Sn was 5*p*-block metal element, but for Bi_2InTaO_7, Ta was 5*d*-block metal element, and In was 5*p*-block metal element, indicating that the crystal structure and the electronic structure of the photocatalysts affect the photocatalytic activity. Based on above analysis, the difference of photocatalytic MB degradation between Bi_2SnTiO_7 and Bi_2InTaO_7 can be attributed mainly to the difference in their crystalline structure and electronic structure. The crystal structure and the electronic structure of the polyaniline-hybridized Bi_2SnTiO_7 and N-doped TiO_2 were totally different. For N-doped TiO_2, Ti was 3*d*-block metal element, indicating that the different photodegradation effect of MB between the polyaniline-hybridized Bi_2SnTiO_7 and N-doped TiO_2 could be attributed mainly to the difference of their crystalline structure and electronic structure.

The present results indicated that the polyaniline-hybridized Bi_2SnTiO_7-visible light photocatalysis system might be regarded as a practical method for treatment of diluted colored waste water. This system could be utilized for decolorization, purification and detoxification of textile, printing and dyeing industries in the long-day countries. Meanwhile, this system did not need high pressure of oxygen, heating or any chemical reagents. Much decolorized and detoxified water were flowed from our new system for treatment, and the results showed that the polyaniline-hybridized Bi_2SnTiO_7-visible light photocatalysis system might provide a valuable treatment for purifying and reusing colored aqueous effluents.

4. Conclusions

The polyaniline-hybridized Bi_2SnTiO_7 was prepared by chemical oxidation in-situ polymerization method and sol-gel method for the first time. The structural and photocatalytic properties of the polyaniline-hybridized Bi_2SnTiO_7 were investigated. XRD results indicated that Bi_2SnTiO_7 crystallized with the pyrochlore-type structure, cubic crystal system and space group *Fd3m*. The lattice parameter of Bi_2SnTiO_7 was found to be a = 10.52582(8) Å. Photocatalytic decomposition of aqueous MB was realized under visible light irradiation in the presence of the polyaniline-hybridized Bi_2SnTiO_7, Bi_2InTaO_7 or N-doped TiO_2. The results showed that the polyaniline-hybridized Bi_2SnTiO_7 owned higher catalytic activity compared with pure TiO_2, Bi_2InTaO_7 or N-doped TiO_2 for photocatalytic degradation of MB under visible light irradiation. The photocatalytic degradation of MB with the polyaniline-hybridized Bi_2SnTiO_7, Bi_2InTaO_7or N-doped TiO_2 as catalyst followed the first-order reaction kinetics, and the first-order rate constant was 0.01504 min^{-1} or 0.00275 min^{-1} or 0.00333 min^{-1}. Complete removal and mineralization of MB was observed after visible light irradiation for 220 min with the polyaniline-hybridized Bi_2SnTiO_7 as catalyst. The reduction of the total organic carbon, the formation of inorganic products such as SO_4^{2-} and NO_3^-, and the evolution of CO_2 revealed the continuous mineralization of MB during the photocatalytic process. The possible photocatalytic degradation pathway of MB was obtained under visible light irradiation. The polyaniline-hybridized Bi_2SnTiO_7/(visible light) photocatalysis system was found to be suitable for textile industry wastewater treatment and could be utilized to solve other environmental chemical pollution problems.

Acknowledgement

This work was supported by the National Natural Science Foundation of China (No.20877040). This work was supported by a grant from the Technological Supporting Foundation of Jiangsu Province (No. BE2009144). This work was supported by a grant from China-Israel Joint Research Program in Water Technology and Renewable Energy (No. 5). This work was supported by a grant from New Technology and New Methodology of Pollution Prevention Program From Enviromental Protection Department of Jiangsu Province of China during 2010 and 2012 (No. 201001). This work was supported by a grant from The Fourth Technological Development Scheming (Industry) Program of Suzhou City of China from 2010 (SYG201006). This work was supported by a grant from the Fundamental Research Funds for the Central Universities.

References

[1] Yazdanbakhsh, M.; Khosravi, I.; Goharshadi, E.K.; Youssefi, A. Fabrication of nanospinel $ZnCr_2O_4$ using sol-gel method and its application on removal of azo dye from aqueous solution. *J. Hazard. Mater.* **2010,** *184 (1-3)*, 684–689.

[2] Cardoso, N.F.; Lima, E.C.; Pinto, I.S.; Amavisca, C.V.; Royer, B.; Pinto, R.B.; Alencar, W.S.; Pereira, S.F.P. Application of cupuassu shell as biosorbent for the removal of textile dyes from aqueous solution. *J. Environ. Manage.* **2011,** *92 (4),* 1237-1247.

[3] Safarik, I.; Horska, K.; Safarikova, M. Magnetically modified spent grain for dye removal. *J. Cereal Sci.* **2011,** *53 (1)*, 78-80.

[4] Nasuha, N.; Hameed, B.H. Adsorption of methylene blue from aqueous solution onto NaOH-modified rejected tea. *Chem. Eng. J.* **2011,** *166 (2)*, 783-786.

[5] Safarik, I.; Rego, L.F.T.; Borovska, M.; Mosiniewicz-Szablewska, E.; Weyda, F.; Safarikova, M. New magnetically responsive yeast-based biosorbent for the efficient removal of water-soluble dyes. *Enzyme Microb. Technol.* **2007,** *40 (6)*, 1551-1556.

[6] Akpan, U.G.; Hameed, B.H. Parameters affecting the photocatalytic degradation of dyes using TiO_2-based photocatalysts: A review. *J. Hazard. Mater.* **2009,** *170 (2-3)*, 520-529.

[7] Valenzuela, M.A.; Bosch, P.; Jiménez-Becerrill, J.; Quiroz, O.; Páez, A.I. Preparation, characterization and photocatalytic activity of ZnO, Fe_2O_3 and $ZnFe_2O_4$. *J. Photochem. Photobiol. A* **2002,** *148 (1-3)*, 177–182.

[8] Yu, H.; Irie, H.; Shimodaira, Y.; Hosogi, Y.; Kuroda, Y.; Miyauchi, M.; Hashimoto, K. An efficient visible-light-sensitive Fe(III)-grafted TiO_2 photocatalyst. *J. Phys. Chem. C* **2010,** *114 (39)*, 16481–16487.

[9] Kitano, S.; Hashimoto, K.; Kominami, H. Photocatalytic degradation of 2-propanol under irradiation of visible light by nanocrystalline titanium(IV) oxide modified with rhodium ion using adsorption method. *Chem. Lett.* **2010,** *39 (6)*, 627-629.

[10] Fan, G.L.; Gu, Z.J.; Yang, L.; Li, F. Nanocrystalline zinc ferrite photocatalysts formed using the colloid mill and hydrothermal technique. *Chem. Eng. J.* **2009,** *155 (1-2)*, 534–541.

[11] Cao, S.W.; Zhu, Y.J.; Cheng, G.F.; Huang, Y.H. $ZnFe_2O_4$ nanoparticles: microwave-hydrothermal ionic liquid synthesis and photocatalytic property over phenol. *J. Hazard. Mater.* **2009,** *171 (1-3)*, 431–435.

[12] Shanmugam, S.; Gabashvili, A.; Jacob, D.S.; Yu, J.C.; Gedanken, A. Synthesis and characterization of TiO_2@C core-shell composite nanoparticles and evaluation of their photocatalytic activities. *Chem. Mater.* **2006,** *18 (9)*, 2275-2282.

[13] Irie, H.; Shibanuma, T.; Kamiya, K.; Miura, S.; Yokoyama, T.; Hashimoto, K. Characterization of Cr(III)-grafted TiO_2 for photocatalytic reaction under visible light. *Appl. Catal. B* **2010,** *96 (1-2)*, 142–147.

[14] Fuku, K.; Hashimoto, K.; Kominami, H. Photocatalytic reductive dechlorination of chlorobenzene to benzene in 2-propanol suspension of metal-loaded titanium(IV) oxide nanocrystals in the presence of dissolved sodium hydroxide. *Chem. Commun.* **2010,** *46 (28)*, 5118–5120.

[15] Selvan, R.K.; Gedanken, A.; Anilkumar, P.; Manikandan, G.; Karunakaran, C. Synthesis and characterization of rare earth orthovanadate (RVO_4; R = La, Ce, Nd, Sm, Eu & Gd) nanorods/nanocrystals/nanospindles by a facile sonochemical method and their catalytic properties. *J. Cluster Sci.* **2009,** *20 (2)*, 291–305.

[16] Waldmann, N.S.; Paz, Y. Photocatalytic reduction of Cr(VI) by titanium dioxide coupled to functionalized CNTs: An example of counterproductive charge separation. *J. Phys. Chem. C* **2010,** *114 (44)*, 18946–18952.

[17] Imanishi, M.; Hashimoto, K.; Kominami, H. Homogeneous photocatalytic mineralization of acetic acid in an aqueous solution of iron ion. *Appl. Catal. B* **2010,** *97 (1-2)*, 213–219.

[18] Zhang, W.W.; Zhang, J.Y.; Chen, Z.Y. Wang, T.M. Photocatalytic degradation of methylene blue by $ZnGa_2O_4$ thin films. *Catal. Commun.* **2009,** *10 (13)*, 1781–1785.

[19] Zhang, W.W.; Zhang, J.Y.; Lan, X.; Chen, Z.Y.; Wang, T.M. Photocatalytic performance of $ZnGa_2O_4$ for degradation of methylene blue and its improvement by doping with Cd. *Catal. Commun.* **2010,** *11 (14)*, 1104–1108.

[20] Tang, J.W.; Zou, Z.G.; Ye, J.H. Effects of substituting Sr^{2+} and Ba^{2+} for Ca^{2+} on the structural properties and photocatalytic behaviors of $CaIn_2O_4$. *Chem. Mater.* **2004,** *16 (9)*, 1644-1649.

[21] Tang, J.W.; Zou, Z.G.; Yin, J.; Ye, J.H. Photocatalytic degradation of methylene blue on $CaIn_2O_4$ under visible light irradiation. *Chem. Phys. Lett.* **2003**, *382 (1-2)*, 175–179.

[22] Tayade, R.J.; Natarajan, T.S.; Bajaj, H.C. Photocatalytic degradation of methylene blue dye using ultraviolet light emitting diodes. *Ind. Eng. Chem. Res.* **2009,** *48 (23)*, 10262–10267.

[23] Chen, C.H.; Liang, Y.H.; Zhang, W.D. $ZnFe_2O_4$/MWCNTs composite with enhanced photocatalytic activity under visible-light irradiation. *J. Alloys Compd.* **2010,** *501 (1)*, 168–172.

[24] Cui, B.; Lin, H.; Liu, Y.Z.; Li, J.B.; Sun, P.; Zhao, X.C.; Liu, C.J. Photophysical and photocatalytic properties of core-ring structured $NiCo_2O_4$ nanoplatelets. *J. Phys. Chem. C* **2009,** *113 (32)*, 14083–14087.

[25] Zhang, H.R.; Tan, K.Q.; Zheng, H.W.; Gu, Y.Z.; Zhang, W.F. Preparation, characterization and photocatalytic activity of TiO_2 codoped with yttrium and nitrogen. *Mater. Chem. Phys.* **2011,** *125 (1-2)*, 156-160.

[26] **Luan, J.F.;** Wang, S.; Ma, K.; Li, Y.M.; Pan, B.C. Structural property and catalytic activity of new In_2YbSbO_7 and Gd_2YbSbO_7 nanocatalysts under visible light irradiation. *J. Phys. Chem. C* **2010,** *114 (20)*, 9398-9407.

[27] Kitano, M.; Takeuchi, M.; Matsuoka, M.; Thomas, J.M.; Anpo, M. Preparation of visible light-responsive TiO_2 thin film photocatalysts by an RF magnetron sputtering deposition method and their photocatalytic reactivity. *Chem. Lett.* **2005,** *34 (4)*, 616-617.

[28] Anpo, M.; Takeuchi, M. The design and development of highly reactive titanium oxide photocatalysts operating under visible light irradiation. *J. Catal.* **2003,** *216 (1-2)*, 505-516.

[29] Hamadanian, M.; Reisi-Vanani, A.; Majedi, A. Preparation and characterization of S-doped TiO_2 nanoparticles, effect of calcination temperature and evaluation of photocatalytic activity. *Mater. Chem. Phys.* **2009,** *116*, 376-382.

[30] Luan. J.F.; Zhao, W.; Feng, J.W.; Cai, H.L.; Zheng, Z.; Pan, B.C.; Wu, X.S.; Zou, Z.G.; Li, Y.M. Structural, photophysical and photocatalytic properties of novel Bi_2AlVO_7. *J. Hazard. Mater.* **2009,** *164 (2-3)*, 781-789.

[31] Marugán, J.; Hufschmidt, D.; Sagawe, G.; Selzer, V.; Bahnemann, D. Optical density and photonic efficiency of silica-supported TiO_2 photocatalysts. *Water Res.* **2006,** 40 (4), 833-839.

[32] Sakthivel, S.; Shankar, M.V.; Palanichamy, M.; Arabindoo, B.; Bahnemann, D.W.; Murugesan, V.; Enhancement of photocatalytic activity by metal deposition: characterisation and photonic efficiency of Pt, Au and Pd deposited on TiO_2 catalyst. *Water Res.* **2004,** *38 (13)*, 3001-3008.

[33] Izumi, F. A software package for the rietveld analysis of X-ray and neutron diffraction patterns. *J. Crystallogr. Assoc. Japan.* **1985,** *27*, 23-26.

[34] Zou, Z.G.; Ye, J.H.; Arakawa, H. Preparation, structural and photophysical properties of Bi_2InNbO_7 compound. *J. Mater. Sci. Lett.* **2000,** *19 (21)*, 1909-1911.

[35] Liu, G.M.; Wu, T.X.; Zhao, J.C.; Hidaka, H.; Serpone, N. Photoassisted degradation of dye pollutants. 8. Irreversible degradation of alizarin red under visible light radiation in air-equilibrated aqueous TiO_2 dispersions. *Environ. Sci. Technol.* **1999,** *33 (12)*, 2081-2087.

[36] Lachheb, H.; Puzenat, E.; Houas, A.; Ksibi, M.; Elaloui, E.; Guilard, C.; Herrmann, J.M. Photocatalytic degradation of various types of dyes (Alizarin S, Crocein Orange G, Methyl Red, Congo Red, Methylene Blue) in water by UV-irradiated titania. *Appl. Catal. B* **2002,** *39 (1)*, 75-90.

[37] Nasr, C.; Vinodgopal, K.; Fisher, L.; Hotchandani, S.; Chattopadhyay, A.K.; Kamat, P.V. Environmental photochemistry on semiconductor surfaces. Visible light induced degradation of a textile diazo dye, naphthol blue black, on TiO_2 nanoparticles. *J. Phys. Chem.* **1996,** *100 (20)*, 8436-8442.

[38] Wiegel, M.; Middel, W.; Blasse, G. Influence of NS_2 ions on the luminescence of niobates and tantalates. *J. Mater. Chem.* **1995,** *5 (7)*, 981-983.

Figure 1. TEM image of Bi_2SnTiO_7 (a) and the selected area electron diffraction pattern of Bi_2SnTiO_7 (b).

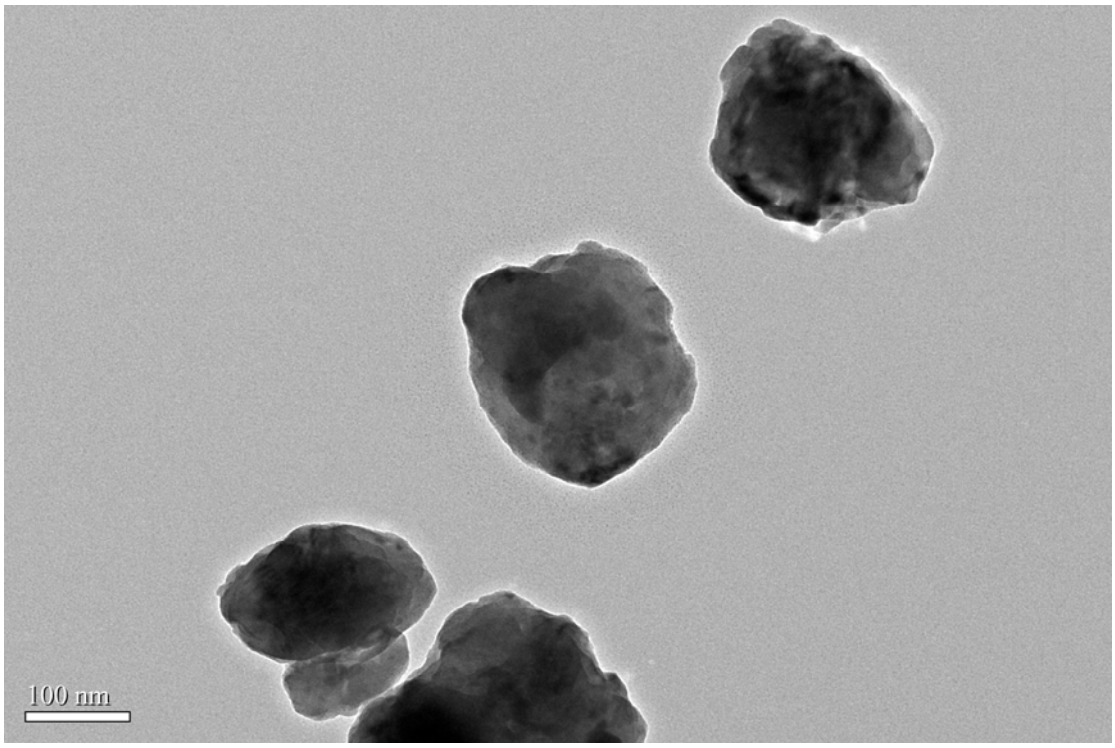

(a)

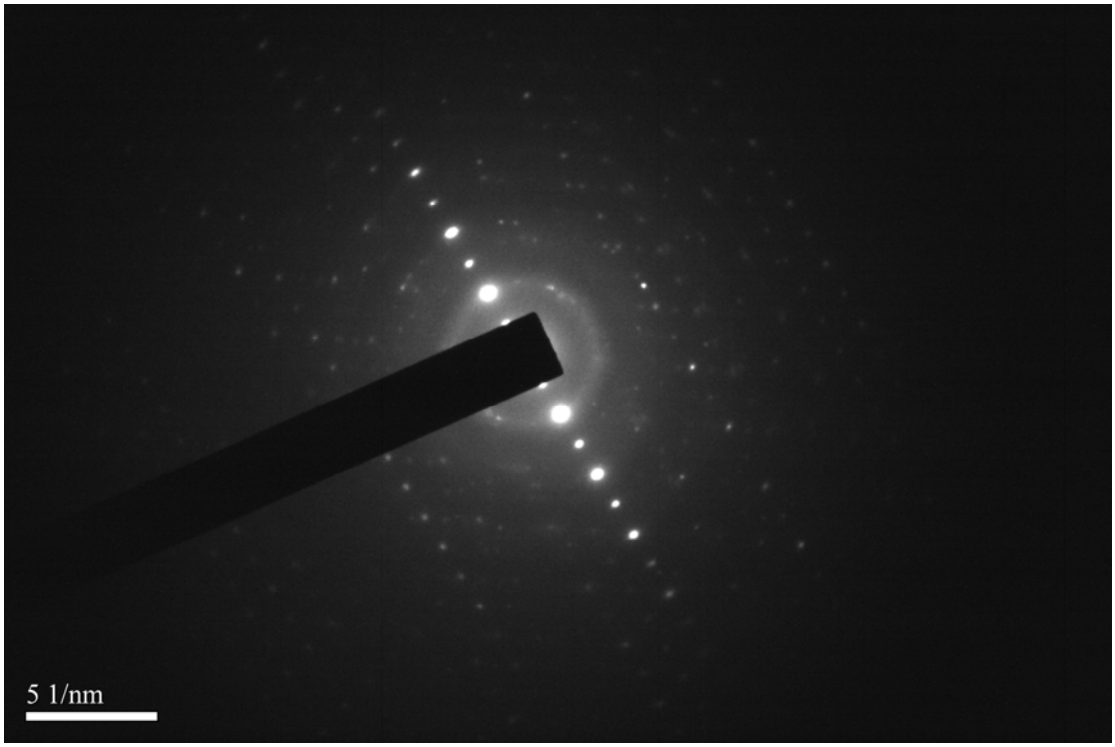

(b)

Figure 2. X-ray powder diffraction pattern and Rietveld refinements of Bi_2SnTiO_7 prepared by a solid-state reaction method at 1100 ^oC. (The experimental X-ray diffraction pattern (—), the simulation X-ray diffraction pattern (×××), the reflection positions (||||), the difference (observed–calculated) profile (·····).)

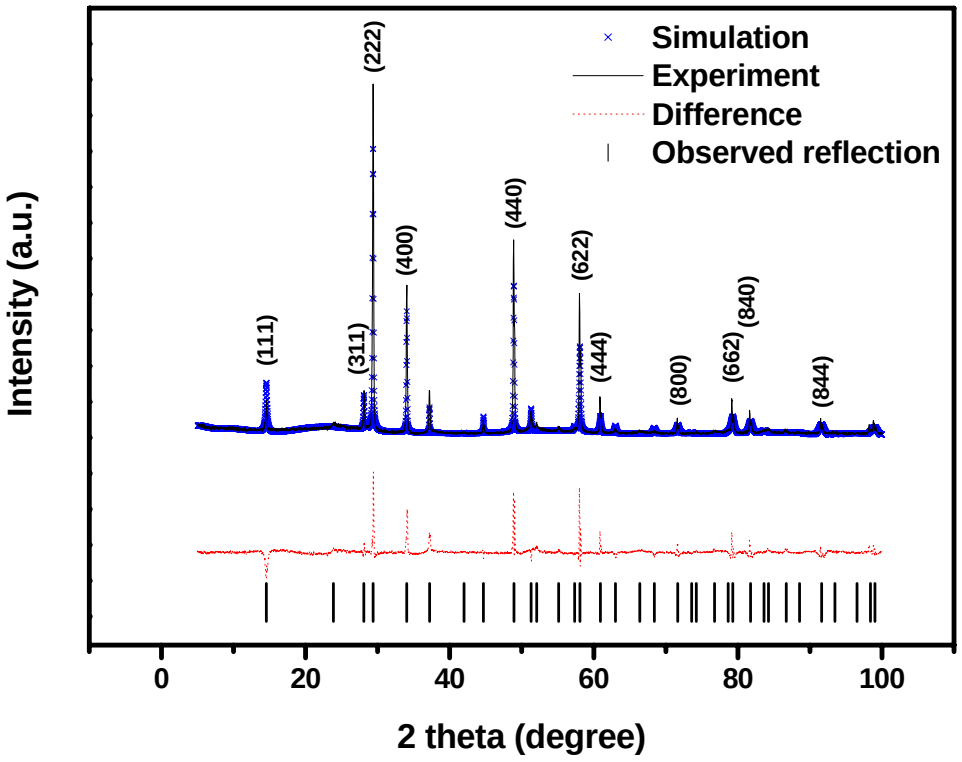

Figure 3. Photocatalytic degradation of methylene blue under visible light irradiation in the presence of the polyaniline-hybridized Bi_2SnTiO_7, Bi_2InTaO_7, pure TiO_2, N-doped TiO_2 as well as in the absence of a photocatalyst.

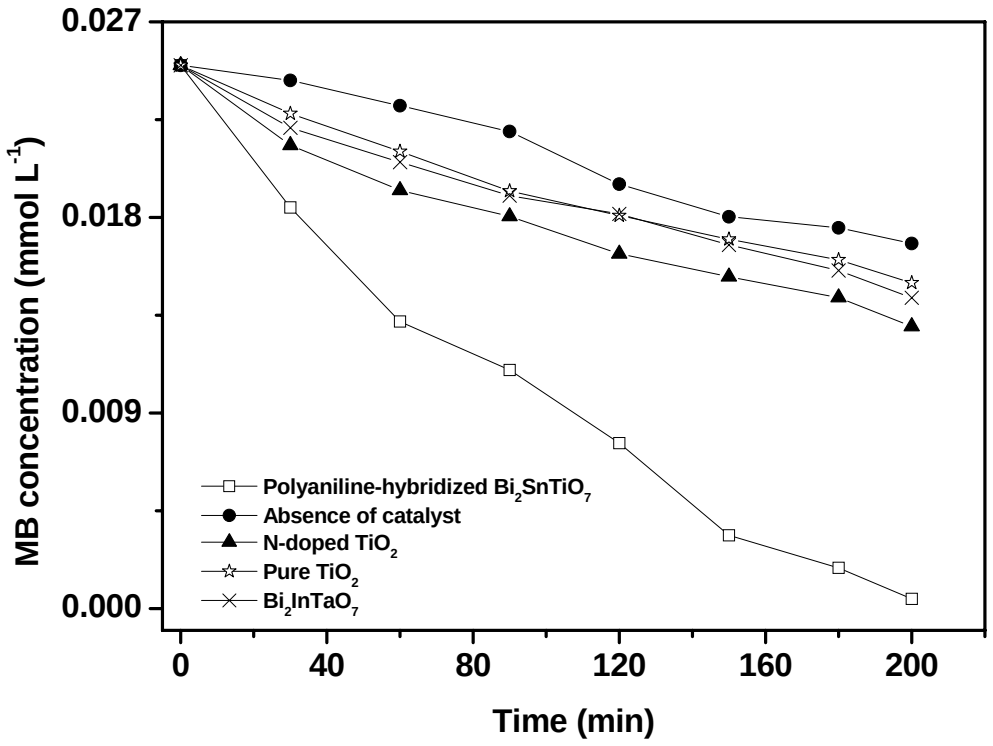

Figure 4. Disappearance of total organic carbon (TOC) during photocatalytic degradation of methylene blue with the polyaniline-hybridized Bi_2SnTiO_7, Bi_2InTaO_7 or N-doped TiO_2 as catalyst under visible light irradiation.

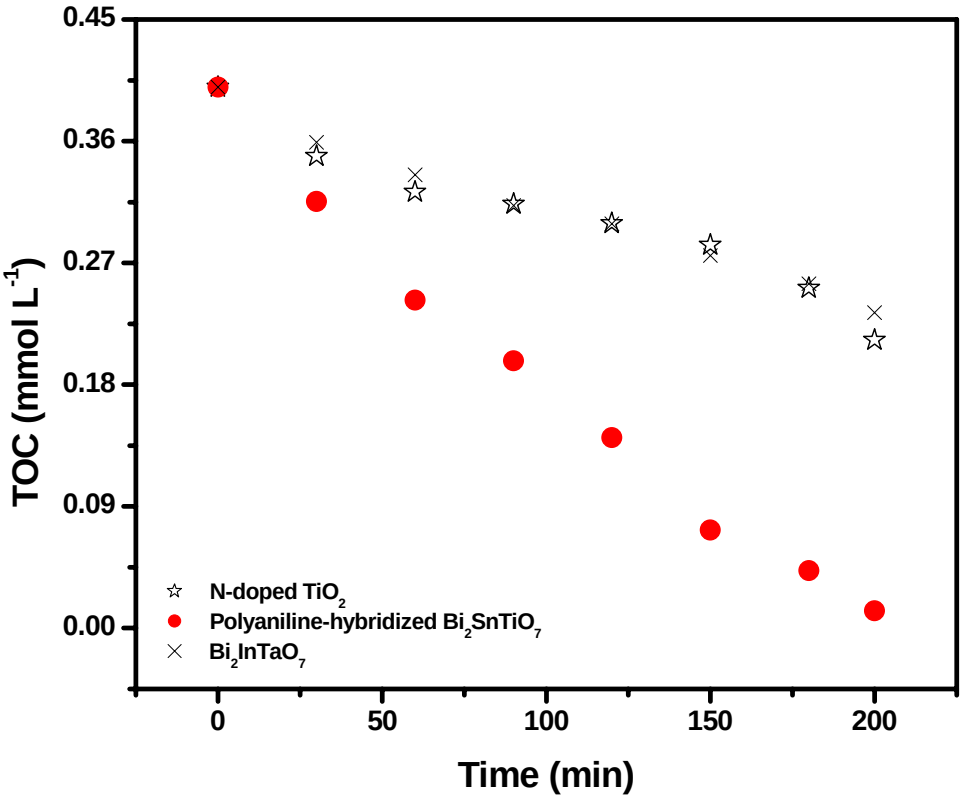

Figure 5. CO_2 production kinetics during the photocatalytic degradation of methylene blue with the polyaniline-hybridized Bi_2SnTiO_7, Bi_2InTaO_7 or N-doped TiO_2 as catalyst under visible light irradiation.

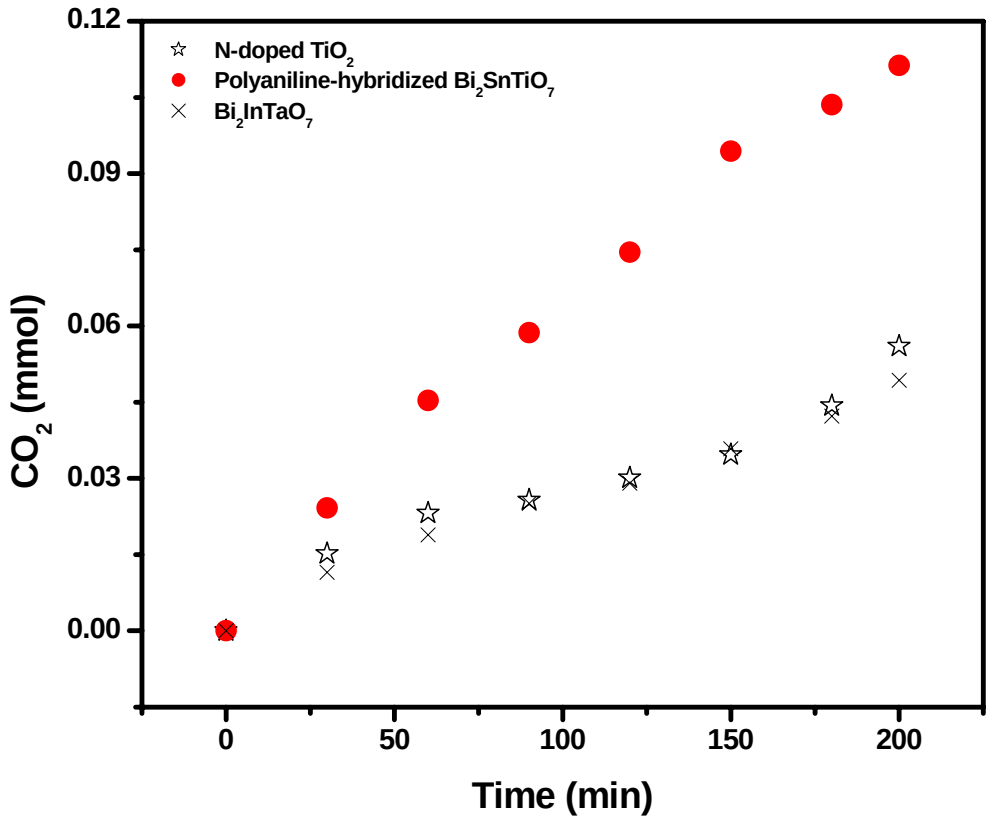

Figure 6. Observed first-order kinetic plots for the photocatalytic degradation of methylene blue with the polyaniline-hybridized Bi_2SnTiO_7, Bi_2InTaO_7 or N-doped TiO_2 as catalyst under visible light irradiation.

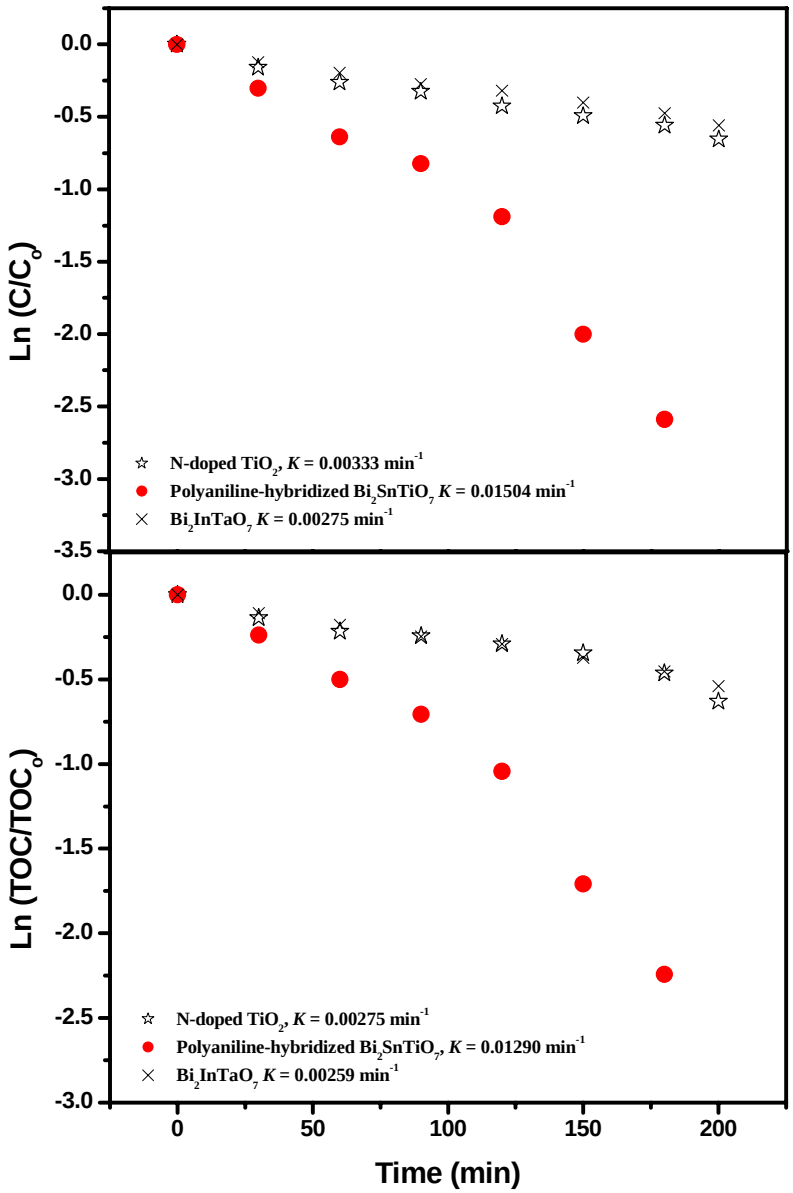

Figure 7. The concentration variation of SO_4^{2-} during photocatalytic degradation of methylene blue with the polyaniline-hybridized Bi_2SnTiO_7, Bi_2InTaO_7 or N-doped TiO_2 as catalyst under visible light irradiation.

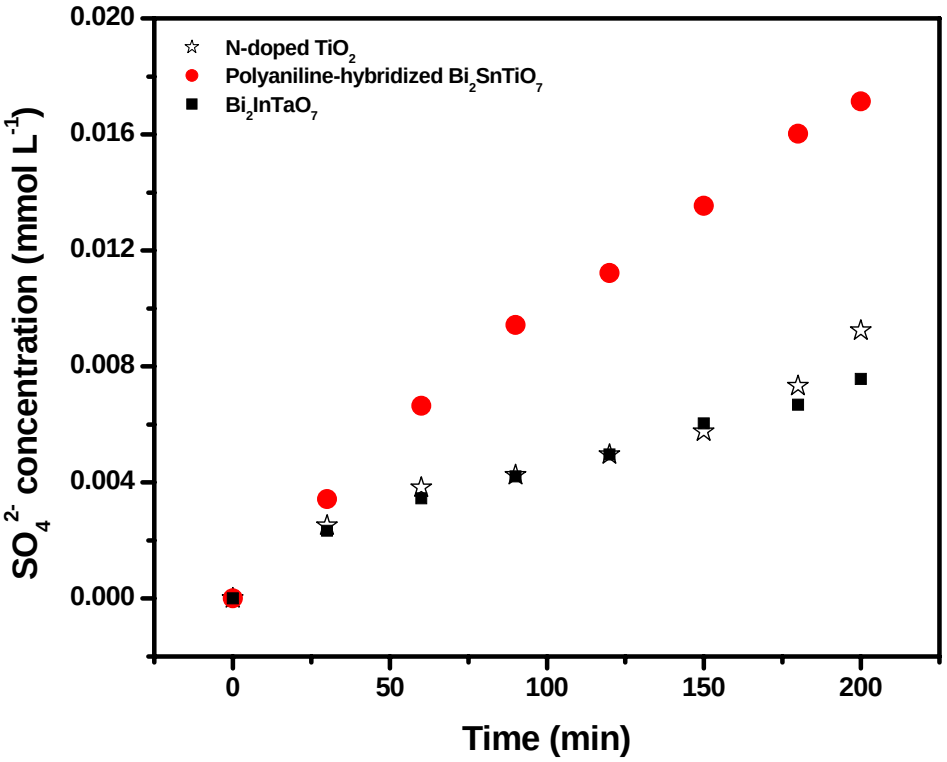

Figure 8. The concentration variation of NO_3^- during photocatalytic degradation of methylene blue with the polyaniline-hybridized Bi_2SnTiO_7, Bi_2InTaO_7 or N-doped TiO_2 as catalyst under visible light irradiation.

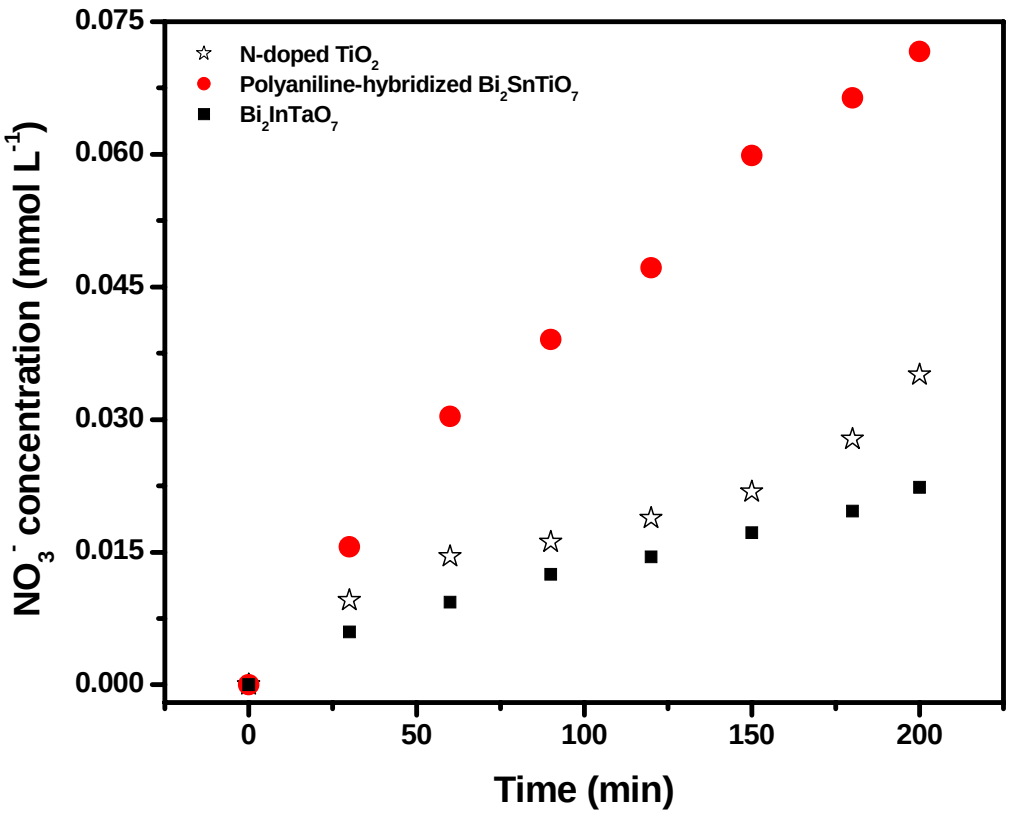

Figure 9. Suggested photocatalytic degradation pathway scheme for methylene blue under visible light irradiation in the presence of the polyaniline-hybridized Bi_2SnTiO_7.

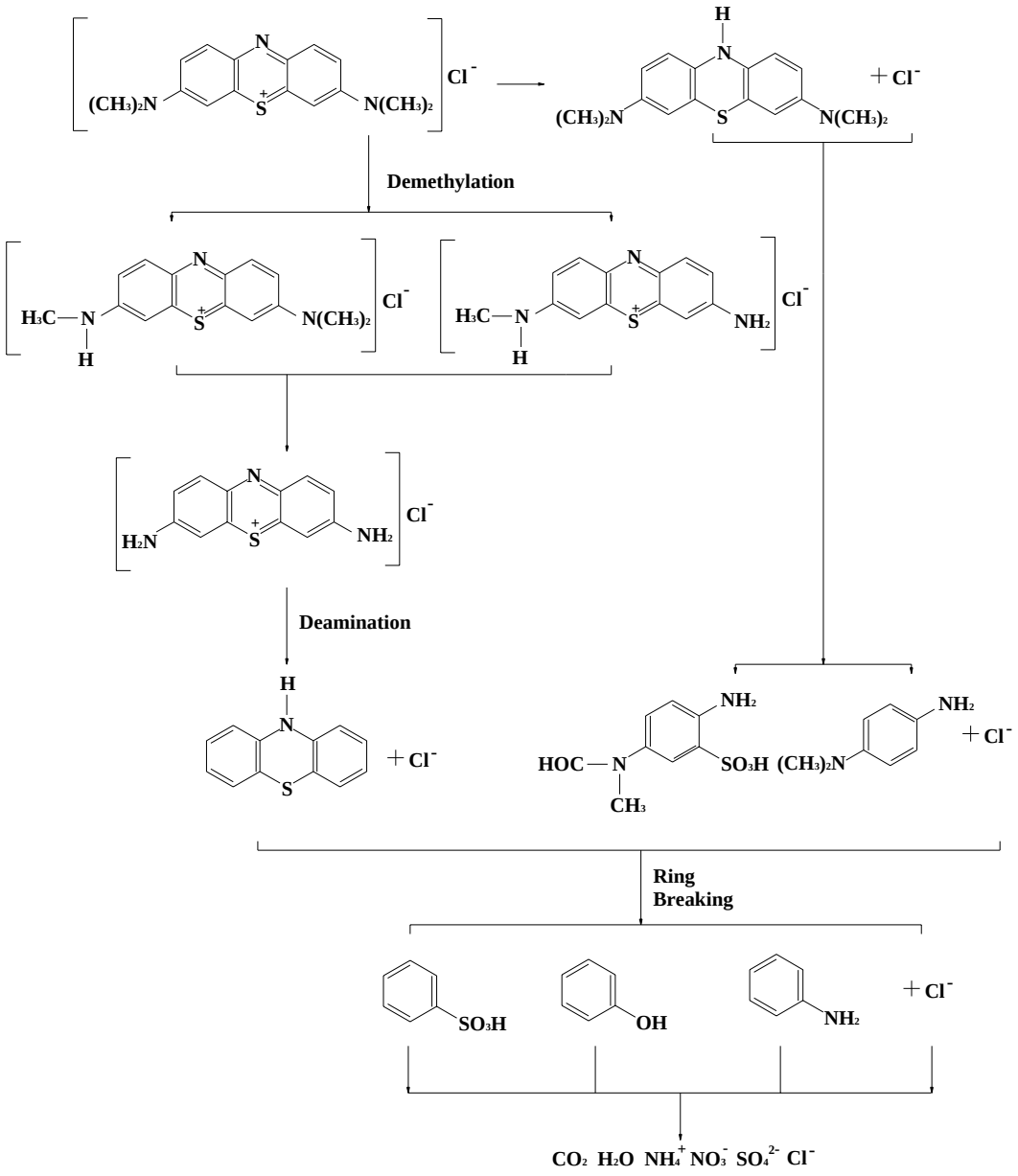

Table 1. Atomic coordinates and structural parameters of Bi_2SnTiO_7 prepared by the solid state reaction method.

Atom	x	y	z	Occupation factor
Bi	0.0000	0	0	1.0
Sn	0.5000	0.5000	0.5000	0.5
Ti	0.5000	0.5000	0.5000	0.5
O(1)	-0.0947	0.1250	0.1250	1.0
O(2)	0.1250	0.1250	0.1250	1.0

Table 2. Binding energies (BE) for key elements from Bi_2SnTiO_7.

Compound	$Bi_{4f7/2}$ BE (eV)	$Sn_{3d5/2}$ BE (eV)	Ti_{3p} BE (eV)	O_{1s} BE (eV)
Bi_2SnTiO_7	159.50	486.55	37.50	530.15